Prediction of the formation of stable periodic self-interstitial cluster chains $[(I_4)_m, m=1-4]$ in Si under biaxial strain

Robert J. Bondi, Sangheon Lee, and Gyeong S. Hwang[a)]
Department of Chemical Engineering, University of Texas, Austin, Texas 78712, USA

(Received 30 March 2009; accepted 9 June 2009; published online 30 June 2009)

Using density functional theory calculations, we examined the structure and stability of extendable self-interstitial cluster configurations $(I_n, n=12,16)$ with four-atom periodicity in crystalline silicon under biaxial strain $(-4\% \leq \varepsilon \leq 4\%)$ on Si(100). In the absence of strain, the ground state configurations of I_{12} and I_{16} share a common structure (I_{12}-like) with C_{2h} symmetry and a four-atom repeating unit; however, we identified an extended configuration based on I_4 (D_{2d} symmetry) cluster aggregates $[(I_4)_m(m=3,4)]$ along $\langle 110 \rangle$ that is more favorable under certain magnitudes of strain. While both the I_{12}-like and $(I_4)_m$ configurations exhibit relative stabilities that are a function of both strain and orientation, the larger $(I_4)_m$ orientation effect is the primary reason that these structures are preferred in both highly tensile and highly compressive environments. This suggests that I_4 derivatives may participate in the growth transition of Si self-interstitial clusters in the compact-to-extended size regime $(10 \leq n \leq 20)$ under strain. © *2009 American Institute of Physics*.
[DOI: 10.1063/1.3160545]

Manufacturing processes to fabricate complementary metal oxide semiconductor (CMOS) transistors will likely rely on increasingly complicated ion implantation processes for the foreseeable future to precisely control dopant concentration profiles in Si. Ion implantation is responsible for the accumulation of excess Si self-interstitials near the projected ion range depth that are associated with both transient-enhanced diffusion of dopants during postimplantation annealing and the evolution of various extended defects.[1–4] While deep-level transient spectroscopy[5] and photoluminescence[2] spectroscopy have evidenced the existence of small interstitial clusters in ion-implanted Si, theoretical studies continue in an effort to better comprehend their behavior.

Strain engineering was widely adopted in the semiconductor industry in the 90 nm technology node as a low-cost, easily integrated method to extend the electrical performance of CMOS transistors in accordance with Moore's Law.[6] Biaxial strain, which is also known as global or bulk strain,[7] is one way to apply strain to the channel of a MOS field effect transistor (MOSFET). Device applications for biaxial strain in Si include heterojunction bipolar transistors[8] and fully depleted CMOS devices using strained silicon on insulator substrates.

In this letter, we discuss the effect that biaxial strain has on the growth behavior of self-interstitial defects using first principles calculations. In particular, the stable I_4 cluster can aggregate with other I_4 clusters to form conditionally stable extended chains that are energetically more favorable than known configurations of the same size under sufficient strain conditions. Our theoretical framework is intended to model the uniform biaxial strain field that might occur in a MOSFET $\langle 110 \rangle$-aligned channel built on a Si (100) wafer orientation. Unless noted otherwise, "strain" in this letter refers to biaxial strain on Si (100).

[a)]Author to whom correspondence should be addressed. Electronic mail: gshwang@che.utexas.edu.

All atomic structures and energies reported herein were calculated using a plane-wave basis set pseudopotential method within the generalized gradient approximation of Perdew and co-workers (GGA-PW91)[9,10] to density functional theory (DFT),[11] as implemented in the well-established Vienna *ab initio* simulation package (VASP).[12] Vanderbilt-type ultrasoft pseudopotentials[13] were used for core-electron interactions. Outer electron wave functions were expanded using a plane-wave basis set with a kinetic energy cutoff of 160 eV. Brillouin zone sampling was performed with one k-point (Γ) for geometric optimization. The geometric optimization allowed all atoms to relax until the total energy had converged within 1×10^{-3} eV tolerance. With the optimized ionic positions determined, corresponding total energies were reevaluated using the $(2\times2\times2)$ Monkhorst–Pack grid. For the strain-free supercell, we used a fixed Si lattice constant (a_{Si}) of 5.457 Å along $\langle 100 \rangle$ or 3.859 Å along $\langle 110 \rangle$ as obtained from volume optimization. Care was taken to ensure that each supercell size is large enough to accommodate a given interstitial cluster with no significant interaction with its periodic images (all supercell sizes are listed in Fig. 3).

From linear elastic theory,[14–17] the relationship between out-of-plane and in-plane strain for a cubic crystal under biaxial strain can be calculated in terms of two tabulated elastic stiffness constants (C_{ij}) (Ref. 18): $\nu^* = -\varepsilon_\perp/\varepsilon_\parallel = 2(C_{12}/C_{11}) = 0.771$. Figure 1(a) depicts how biaxial strain is modeled in our crystalline Si system. Using $\nu^*=0.771$, $\varepsilon_\parallel = (a_\parallel - a_{\mathrm{Si}})/a_{\mathrm{Si}}$, and $\varepsilon_\perp = (a_\perp - a_{\mathrm{Si}})/a_{\mathrm{Si}}$, we calculated the values of out-of-plane a_{Si} ($a_\perp$) for each independent value of in-plane a_{Si} ($a_\parallel$) studied. The range of biaxial strain investigated $(-4\% \leq \varepsilon \leq 4\%)$ is based on the limiting tensile case for Si ($a_{\mathrm{Si}} = 5.4309$ Å) (Ref. 16) grown on pure Ge ($a_{\mathrm{Ge}} = 5.6461$ Å).[16] For each biaxial strain condition, we created a unique supercell with dimensions scaled using ν^*.

We evaluated formation energies to estimate relative cluster stability among various configurations and orienta-

 © 2009 American Institute of Physics

Downloaded 02 Sep 2010 to 146.6.194.60. Redistribution subject to AIP license or copyright; see http://apl.aip.org/about/rights_and_permissions

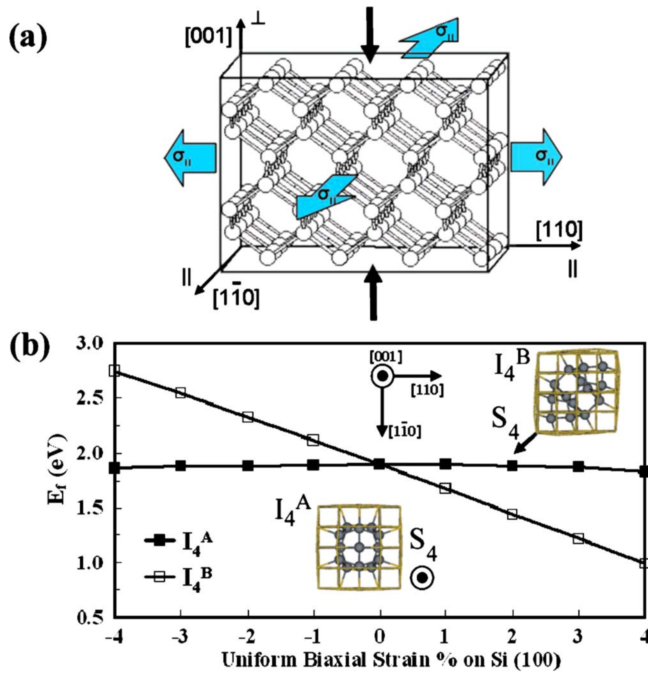

FIG. 1. (Color online) (a) Tensile biaxial stress/strain interaction in our model Si supercell. Applied stress and resulting strain in the plane of the substrate acts equally in all directions (block arrows). In response, the lattice contracts in the out-of-plane direction (black arrows). Under compression, the directions of all arrows are inverted. (b) Formation energy response per interstitial compared for the two relevant orientations of I_4 using $256+n$ supercells. Perspective views along [001] are shown for reference along with corresponding orientations of the S_4 rotation-reflection axes. Light gray (gold) wireframe represents the bulk Si lattice. Dark gray spheres denote interstitials and their highly strained neighbors.

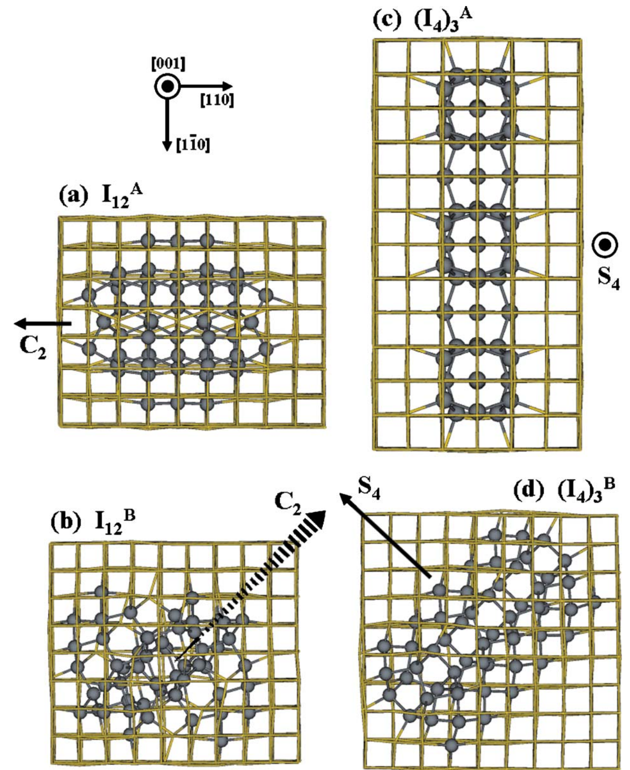

FIG. 2. (Color online) Various embedded configurations and orientations of I_{12} as viewed along [001]. Light gray (gold) wireframe represents the bulk Si lattice. Dark gray spheres denote interstitials and their highly strained neighbors. For (a) I_{12}^A and (b) I_{12}^B, the C_2 axis is shown for each orientation of the ground state configuration with C_{2h} symmetry. For I_{12}^B, the C_2 axis traces a diagonal path through the supercell interior and emerges from the page at a 45° angle. For (c) $(I_4)_3^A$ and (d) $(I_4)_3^B$, the S_4 axis of an individual I_4 core is shown for each I_4-chain configuration.

tions. The formation energy $E_f(n,\varepsilon)$ is given in terms of size (n) and biaxial strain condition (ε) as $E_f(n,\varepsilon)=E_{\text{tot}}(n,\varepsilon)-(n+N)E_{\text{bulk}}(\varepsilon)/N$, where $E_{\text{tot}}(n,\varepsilon)$ is the total energy of the I_n cluster in the $n+N$ atom supercell, n is the size of the interstitial cluster, N is the basis number of atoms in the bulk Si supercell, and $E_{\text{bulk}}(\varepsilon)$ is the total energy of the N atom supercell of crystalline Si at a given biaxial strain condition. We report $E_f(n,\varepsilon)$ on a per interstitial atom basis throughout this letter.

The structural details of the I_4 Si self-interstitial cluster were first reported by Arai *et al.*[19] The recent work of Lee and Hwang[20,21] shows the ground state configuration of I_8 is comprised of two adjacent I_4 cores, where each I_4 core is the same structure detailed by Arai *et al.*[19] Our recent work[22] on strained interstitial clusters reveals that both I_4 and I_8 become more stable under certain strain conditions. The $E_f(4,\varepsilon)$ dependence of I_4 on biaxial strain is determined by the orientation of I_4 with respect to the biaxial strain field as shown in Fig. 1(b) [the $E_f(8,\varepsilon)$ response of I_8 is nearly identical]. Motivated by this interesting behavior observed for I_4 core derivative configurations, we proceeded to search for a potential family of extended configurations composed of I_4 core units using the integrated atomic modeling procedure[20,21] under strained conditions. Starting with the I_8 ground state configuration,[21] four Si interstitials were added in the vicinity and a conditionally stable I_{12} structure was discovered as depicted in Figs. 2(c) and 2(d).

In the previous work of Lee and Hwang,[21] theoretical support is given to delineate Si self-interstitial clustering into three competing regimes based on approximate size and configuration: (1) compact clusters largely based on I_4 derivatives ($n\leq 10$), (2) extended transition configurations ($10\leq n\leq 20$), and (3) defects containing {311} structural cores ($n\geq 20$). In addition, this previous work[21] also identified a configuration family based on the ground state configuration of I_{12} with C_{2h} symmetry that is shown to collectively interrelate the most favorable configurations in the transition regime ($10\leq n\leq 20$).

Figure 2 shows the two relevant orientations[22] (A and B) under biaxial strain of both the I_{12} ground state and I_4 chain configurations. In this work, we also analyzed I_{16} structures that are extensions of the I_{12} structures of Fig. 2. I_{16}^A with C_{2h} symmetry is made by extending I_{12}^A along [110] with a four-atom core repeating unit added to the periodic architecture, while $(I_4)_4^A$ is made by adding an additional I_4 core to $(I_4)_3^A$ along [1$\bar{1}$0] as seen in Fig. 2. While the repeating unit is comprised of four interstitials for both extended transition configurations, note that the repeating unit itself is a different configuration in each case. In order to emphasize the intraconfigurational composition of I_4 cores, we will refer to the I_4 chain configurations as $(I_4)_m$, where m represents the number of I_4 cores in the chain. Similarly, we will collectively refer to the I_{12} and I_{16} ground state configurations as "I_{12}-like" in our discussion.

Figure 3 presents DFT-calculated $E_f(n,\varepsilon)$ data as a function of strain for the relevant orientations of the I_{12}-like and $(I_4)_m$ configurations of both I_{12} and I_{16}. The I_{12}-like configurations exhibit a mild orientation-dependent $E_f(n,\varepsilon)$ re-

Downloaded 02 Sep 2010 to 146.6.194.60. Redistribution subject to AIP license or copyright; see http://apl.aip.org/about/rights_and_permissions

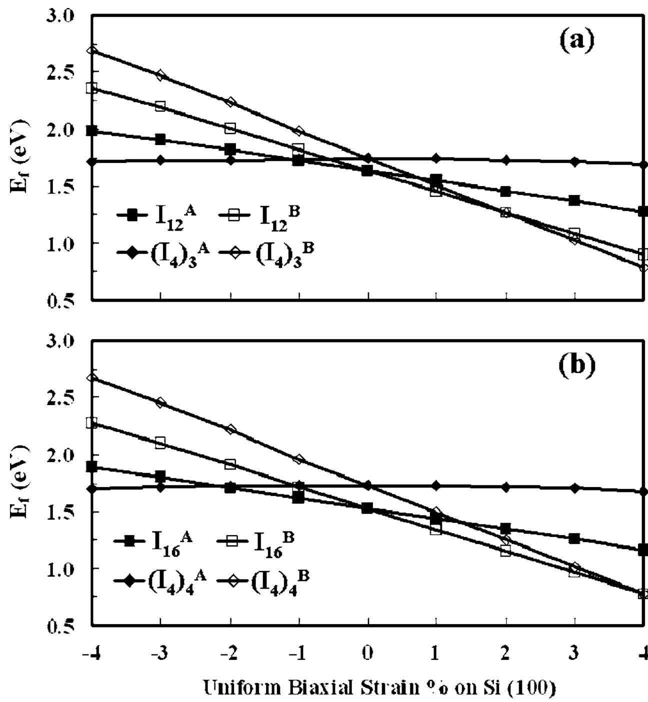

FIG. 3. Formation energy response per interstitial for various configurations and orientations of (a) I_{12} and (b) I_{16} clusters as a function of strain. The elongated shapes of some clusters prompted employment of specialized supercell sizes as follows: $480+n$ [$I_{12}{}^A, I_{12}{}^B$], $576+n$ [$(I_4)_3{}^B$], $640+n$ [$(I_4)_3{}^A$], $672+n$ [$I_{16}{}^A, I_{16}{}^B$], $800+n$ [$(I_4)_4{}^A$], and $840+n$ [$(I_4)_4{}^B$].

sponse to strain, which we have observed as typical behavior for clusters containing significant quantities of split ⟨110⟩-like bonds in their interiors. For the "A" orientations of the I_{12}-like configurations, we see less sensitivity in the $E_f(n,\varepsilon)$ responses to strain relative to the "B" orientations. In analogy with I_4 and I_8, the A orientations of the $(I_4)_m$ configurations show nearly invariant $E_f(n,\varepsilon)$ strain responses for both $(I_4)_3$ and $(I_4)_4$, while the corresponding B orientations show strong $E_f(n,\varepsilon)$ dependence on strain conditions. The main difference in our I_{12}-like results between the $n=12$ case [Fig. 3(a)] and the $n=16$ case [Fig. 3(b)] is simply the strain-free $E_f(n,\varepsilon)$ values [$E_f(n,0)=1.63$ eV (I_{12}) and $E_f(n,0)=1.52$ eV (I_{16})]; in contrast, the $E_f(n,0)$ values for $(I_4)_3$ and $(I_4)_4$ only differ by 10 meV. For both the I_{12}-like and $(I_4)_m$ configurations, the slopes of the $E_f(n,\varepsilon)$ responses as a function of strain are strictly dependent on their respective orientations, not cluster sizes.

It is apparent in Fig. 3 that the $(I_4)_m$ configurations can be energetically favorable in the compact-to-extended transition regime of interstitial cluster growth when strain conditions are present. Using I_{12} as an example [Fig. 3(a)], our results suggest that the preferred configuration/orientation for 12 Si interstitials under biaxial strain ($-4\% \leq \varepsilon \leq 4\%$) could proceed as follows: (1) $(I_4)_3{}^A$ for high compression ($-4\% \leq \varepsilon \leq -1\%$), (2) $I_{12}{}^A$ for low compression ($-1\% \leq \varepsilon \leq 0\%$), (3) $I_{12}{}^B$ for low tension ($0\% \leq \varepsilon \leq 2\%$), and (4) $(I_4)_3{}^B$ for high tension ($2\% \leq \varepsilon \leq 4\%$). Most importantly, the $(I_4)_m$ configuration appears to be the most favorable configuration for the $n=12$ and $n=16$ cluster sizes when the magnitude of biaxial strain is large. Furthermore, the orientation-dependent strain response associated with the D_{2d} symmetry of the I_4 core makes the $(I_4)_m$ configuration energetically preferable under both highly compressive and highly tensile conditions—the sign of biaxial strain will determine the prevalent orientation of $(I_4)_m$. The energy gain of the $(I_4)_m$ configurations over the I_{12}-like configurations is larger under compression than for tension. We can speculate from the trends observed for $n=12$ and $n=16$ that minimum energy configurations for larger clusters ($n>20$) will trend toward the stable configurations experimentally observed in {311} extended defects. Nevertheless, our theoretical results suggest that the $(I_4)_m$ configuration can be prevalent in the compact-to-extended transition regime depending on the cluster size (n) and the magnitude of biaxial strain present.

In summary, we show that the stable I_4 core can aggregate with other I_4 cores along ⟨110⟩ to form short extended defect chains [$(I_4)_m(m=3,4)$] that become more favorable than ground-state, I_{12}-like configurations under sufficient biaxial strain conditions. The prevalent orientations that both $(I_4)_m$ and I_{12}-like elongated configurations will adopt depend on the nature (tensile/compressive) of biaxial strain present, but the larger difference in orientation-dependent relative stability in the $(I_4)_m$ configurations is the main reason that these configurations are preferable under certain strain conditions. Our results suggest that the $(I_4)_m$ configurations may participate in the compact-to-extended transition regime ($10 \leq n \leq 20$) of self-interstitial cluster growth under sufficient strain conditions.

We acknowledge Semiconductor Research Corporation (Grant No. 1413-001), National Science Foundation (Grant No. CAREER-CTS-0449373), and Robert A. Welch Foundation (Grant No. F-1535) for their financial support. We would also like to thank the Texas Advanced Computing Center for use of their computing resources.

[1] J. Kim, F. Kirchhoff, J. W. Wilkins, and F. S. Khan, Phys. Rev. Lett. **84**, 503 (2000).
[2] P. K. Giri, Semicond. Sci. Technol. **20**, 638 (2005).
[3] J. Kim, J. W. Wilkins, F. S. Khan, and A. Canning, Phys. Rev. B **55**, 16186 (1997).
[4] M. Kohyama and S. Takeda, Phys. Rev. B **46**, 12305 (1992).
[5] J. L. Benton, K. Halliburton, S. Libertino, D. J. Eaglesham, and S. Coffa, J. Appl. Phys. **84**, 4749 (1998).
[6] S. E. Thompson, G. Sun, Y. S. Choi, and T. Nishida, IEEE Trans. Electron Devices **53**, 1010 (2006).
[7] K. Derbyshire, Solid State Technol. **50**, 38 (2007).
[8] D. J. Paul, Semicond. Sci. Technol. **19**, R75 (2004).
[9] J. P. Perdew, K. Burke, and M. Ernzerhof, Phys. Rev. Lett. **77**, 3865 (1996).
[10] J. P. Perdew and Y. Wang, Phys. Rev. B **45**, 13244 (1992).
[11] G. Kresse and J. Hafner, Phys. Rev. B **47**, 558 (1993); **49**, 14251 (1994); G. Kresse and J. Furthmuller, Comput. Mater. Sci. **6**, 15 (1996); Phys. Rev. B **54**, 11169 (1996).
[12] G. Kresse and J. Furthmuller, *VASP the Guide* (Vienna University of Technology, Vienna, 2001).
[13] D. Vanderbilt, Phys. Rev. B **41**, 7892 (1990).
[14] L. Lin, T. Kirichenko, B. R. Sahu, G. S. Hwang, and S. K. Banerjee, Phys. Rev. B **72**, 205206 (2005).
[15] P. Bhattacharya, *Semiconductor Optoelectronic Devices* (Prentice Hall, Upper Saddle River, 1997).
[16] J. Singh, *Physics of Semiconductors and Their Heterostructures* (McGraw-Hill, New York, 1993).
[17] C. G. Van de Walle and R. M. Martin, Phys. Rev. B **34**, 5621 (1986).
[18] M. E. Levinshtein, S. L. Rumyantsev, and M. S. Shur, *Handbook Series on Semiconductor Parameters* (World Scientific, London, 1996), Vol. 1, p. 29.
[19] N. Arai, S. Takeda, and M. Kohyama, Phys. Rev. Lett. **78**, 4265 (1997).
[20] S. Lee and G. S. Hwang, Phys. Rev. B **77**, 085210 (2008).
[21] S. Lee and G. S. Hwang, Phys. Rev. B **78**, 045204 (2008).
[22] R. J. Bondi, S. Lee, and G. S. Hwang, Phys. Rev. B **79**, 104106 (2009).

Downloaded 02 Sep 2010 to 146.6.194.60. Redistribution subject to AIP license or copyright; see http://apl.aip.org/about/rights_and_permissions